

The third order optical nonlinear character of ZnSe nanocrystals doped silica glasses

Xing Wan · Xi Yao · Minqiang Wang · Haiyan Hao

Published online: 13 September 2007
© Springer Science + Business Media, LLC 2007

Abstract ZnSe/SiO₂ composites were fabricated with conventional sol–gel synthesis method. The absorption spectra of the semiconductor-doped glasses (SDGs) were presented and compared among different ZnSe doping amounts. The energy gap (E_g) decreased distinctly as the content of ZnSe QDs increased. Nonlinear refractive indexes were measured by single beam Z-scan technique. The results revealed that the third order nonlinear susceptibility was efficiently affected by E_g , which was explained by local field effect and Kramers–Kronig (KK) relation.

Keywords ZnSe · Third order nonlinearity · Local field effect · Kramers–Kronig relations

1 Introduction

Semiconductor doped glasses materials (SDGs) exhibit unique optical and electrical properties, which render them the most popular candidate of optoelectronic devices, nonlinear elements, and optical sensors [1–3]. When the size of QDs is reduced to approach the exciton Bohr radius, the SDGs exhibit intermediate behavior between a bulk crystal and an isolated molecule. Quantum size effects created the blue-shift of the band edge gap and splitting of the electronic states. The magnitude and dispersion of nonlinear refractive index are important in applications such as nonlinear propagation in fibers, fast optical switching, self-focusing and damage in optical materials. CdSe,

ZnS, CdS_xSe_{1-x} [4–6] and some other semiconductor composite materials have been extensively studied. However, there are few third order optical nonlinear index reports about ZnSe SDGs. In fact, ZnSe nanocrystals (NCs) doped SiO₂ composites exhibit nonlinear optical properties comparable with most other SDGs, besides, it reveals a unique optical limiting character [7]. In this text we presented the optical nonlinear coefficients of the ZnSe SDGs. The differences among the samples with different ZnSe content were investigated. Finally, the mechanism and influence factors of the optical nonlinearity were discussed.

2 Experimental details

The synthesis route adopted the conventional sol–gel technique [8, 9]. The gel was first heat treated in air to remove water and organics then a reductive atmosphere to control the NCs size further. The X-ray diffraction pattern and photoluminescence spectrum have already been reported in our earlier theses [7, 9], which validated the QDs dispersed homogenized in the silica glasses. Optical absorption spectra of the samples were recorded on JASCO v-570 spectrometer in the range of 350–800 nm at room temperature. The nonlinear refractive index was characterized by a modified Z-scan technique. A frequency doubled (532 nm) Q-switched Nd:YAG laser (GCR170, Spectrum-Physics, Inc.) with pulse width of 8 ns, beam waist $\omega_0 = 25 \mu\text{m}$ was used to excite the sample. For numerical calculation, the laser pulse was supposed to have a Gaussian profile both spatially and temporally. A lens of 260 mm focal length was used to focus the laser beam onto the tested sample. Input and output energies are measured by two J4-09 series Moletron energy detectors. A step-motor driver is used to move the sample in the direction of

X. Wan · X. Yao · M. Wang (✉) · H. Hao
Electronic Materials Research Laboratory, Key laboratory
of the Ministry of Education, Xi'an Jiaotong University,
Xi'an 710049, China
e-mail: mqwang@mailst.xjtu.edu.cn

light incidence near the focus spot of the lens. The experimental system is controlled by a computer, which includes sample move, energy and transmittance measurement, and laser trigger signal.

3 Results and discussion

Optical absorption spectra of ZnSe QDs doped glasses at room temperature are presented in Fig. 1. The sharp absorption edge indicates a narrow size distribution. The lowest exciton transition energy, considered as the band edge of the SDGs, was calculated with the second derivative spectrum of the absorption spectra. According to the effective mass approximation (EMA), the mean radii of the QDs were estimated as 2.56, 2.58, 2.72 nm, according to the ZnSe content of 1, 2 and 3%. The NCs size increased with the doping amount increased. The exciton Bohr radius of ZnSe is 3.3 nm, so the QDs are in the strong confinement regime.

Prior to Z-scan for the SDGs, we carried out a closed aperture Z-scan measurement on a CS₂ reference sample in a 1 mm length quartz cell. The nonlinear refractive index, n_2 , for CS₂ was $(1.3 \pm 0.3) \times 10^{-11}$ esu, which is fairly consistent with widely accepted values [10, 11]. This proved that the experimental system is credible. In order to reduce the possible thermal accumulative effect we set up the repetition rate to 1 HZ.

Figure 2 shows the typical normalized transmittance versus the sample position (z) measured with closed aperture Z-scan system. The figure exhibits a peak-valley character, which indicates that the third-order nonlinear index is negative. The result is consistent with the bulk ZnSe measured at 532 nm. The solid curves are the fitting results with the following method. As the two photons absorption (TPA) inevitably occurred, the third order

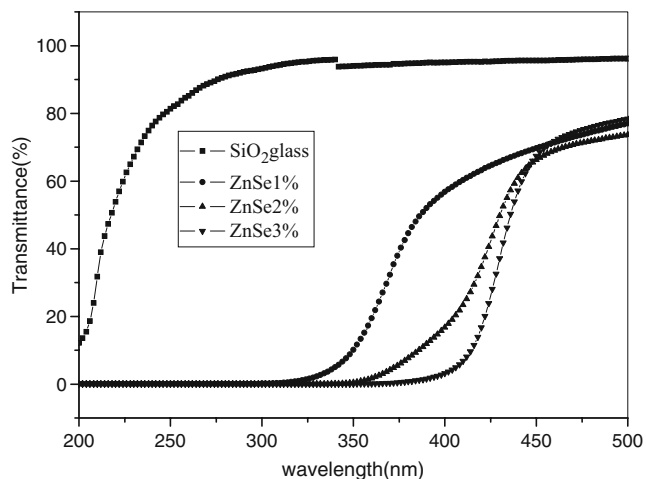


Fig. 1 Absorption spectra of ZnSe doped glasses with ZnSe:SiO₂ molar ratio of 1, 2, 3%

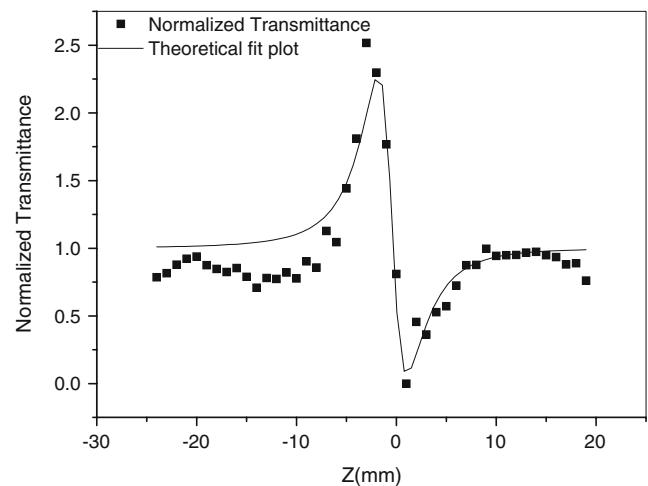


Fig. 2 Closed aperture plot of Z-scan measurement of the ZnSe/SiO₂ composite

nonlinear coefficients were calculated with the following equation [12, 13]:

$$T = 1 - \frac{2(\rho x^2 - 2x + 3\rho)}{(x^2 + 9)(x^2 + 1)} \Delta\Phi \quad (1)$$

$$\rho = \frac{\chi_i^{(3)}}{\chi_R^{(3)}} = \frac{\beta}{2k\gamma} \quad (2)$$

where T is the normalized transmittance, and $\Delta\Phi$ is the nonlinear phase shift due to the nonlinear refraction. $X = Z/Z_0$, $Z_0 = \pi\omega_0/\lambda$ is the diffraction length of the beam, and z is the sample position. The phase shift due to the absorption was taken into account by ρ , so both β and γ can be obtained only by closed aperture Z-scan measurement. It should also be noted that, when other absorptions exist, they are also included in β . The experimental data fitted with the Eq. 1 was exhibited in Table 1. The open aperture Z-scan experimental data of different ZnSe content were also presented (Fig. 3). The solid plots were the fitted results with the equation

$$T(z, S = 1) = \sum_{m=0}^{\infty} \frac{[-q_0(z, 0)]^m}{(m+1)^{3/2}} \text{ for } |q_0| \quad (3)$$

Here the third order nonlinear susceptibility is considered to be a complex quantity, $\chi^{(3)} = \chi_R^{(3)} + i\chi_I^{(3)}$, the imaginary part is related to TPA coefficient β and the real part is related to the nonlinear coefficient γ . The thickness of the samples is below 1 mm, so low intensities of the laser beam could generate detectable optical signal. As the incident laser intensity is in the linear region of the optical limiting curves, the higher order nonlinearity could be avoided. From Table 1 we could know that the third-order nonlinear susceptibility of ZnSe/SiO₂ SDGs is about

Table 1 Third order nonlinear index and energy gap of the ZnSe doped glasses.

	β (cm/Gw)	γ (10^{-18}) (m ² /w)	E _g (ev)	Radius (nm)	n_2 (10^{-11} esu)
ZnSe, 1%	13.8	-1.76	3.40	2.56	-1.14
ZnSe, 2%	14.5	-7.42	3.35	2.58	-4.80
ZnSe, 3%	18.75	-11.5	3.02	2.72	-7.44

10^{-11} esu. For the porous SiO₂, it's about 10^{-14} esu. Moreover, for the same exciting wavelength (532 nm), the nonlinear coefficient γ is larger than that of bulk ZnSe reported before [12]. It could be concluded that the good nonlinear character comes from the structure of ZnSe embedded in SiO₂ network. Compared with n_2 of other typical wide band gap materials CdS [14], CdSe [15] and ZnS [5], ZnSe composites exhibit γ with the same quantitative level. However, as the doping amount and E_g varied, the nonlinear index may be tailored larger or smaller than other materials. Because the wavelength of the laser is 532 nm, the frequency is below the band gap ($h\omega/E_g \approx 0.7$), the enhancement of the nonlinear effect is non-resonant. At resonance, one can take into account just a few dominant electronic states. On the contrary, below the band-gap, the whole set of discrete states must be considered. It's rather difficult to obtain quantitative theoretical predictions for the nonlinearity.

Examination of the data in Table 1 and Fig. 3 revealed a trend, that is as the ratio of ZnSe NCs versus SiO₂ increased, the third order susceptibility enlarged, too. This accorded with the local field effect. The differences in the dielectric constants changed the field distribution inside the nanostructure dramatically. The linear susceptibility of

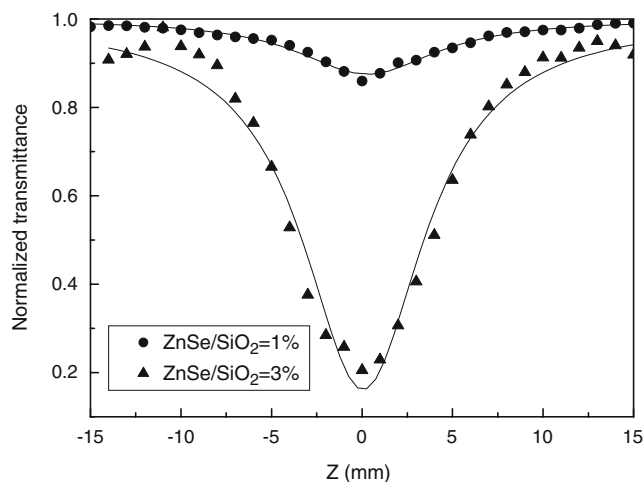


Fig. 3 Open aperture plot of Z-scan measurement of SDGs with different NCs content

semiconductor doped medium composites could be expressed as:

$$\chi_{SDG} = \chi_g + pf(\omega)(\chi_n - \chi_g) \tag{4}$$

p is the volume factor and f is the local field intensity factor. n and g represents the NCs and glass medium respectively. When $\chi_n^{(3)} \gg \chi_g^{(3)}$, the nonlinear susceptibility is

$$\begin{aligned} \chi_{SDG}^{(3)}(\omega_1, -\omega_1, \omega_2) &= \chi_g^{(3)}(\omega_1, -\omega_1, \omega_2) \\ &+ pf^2(\omega_2)|f(\omega_1)|^2\chi_n^{(3)}(\omega_1, -\omega_1, \omega_2) \end{aligned} \tag{5}$$

Generally, $\chi_{SDG} \propto p$. But the relation between volume factor and doping amount is not very distinct here because the dissipation during the fabrication process. So the relation between n_2 and E_g derived from the Kramers–Kronig (KK) relation [16] was applied:

$$Re(\chi^{(3)}) = ME_g^{-4}G_2\left(\frac{h\omega}{E_g}\right) \tag{6}$$

M is a constant, and the function $G_2(y)$ was presented in Fig. 4. The nonlinear susceptibility varies almost with E_g^{-4} . However, we found that for the SDGs, this approximate equation fitted the experimental results when ZnSe content were larger. When the content of ZnSe QDs was very small (1%), the nonlinear coefficients departed from the equation fitted results. This is ascribe to that $G_2(y)$ decreased as the E_g increases when $h\omega/E_g > 0.55$. From the frequency response curves (Fig. 4) we know that n_2 changes with the same trend of $G_2(y)$. For the sample with 1% ZnSe doped, $h\omega/E_g \approx 0.7$, a value at which the sign of $G_2(y)$

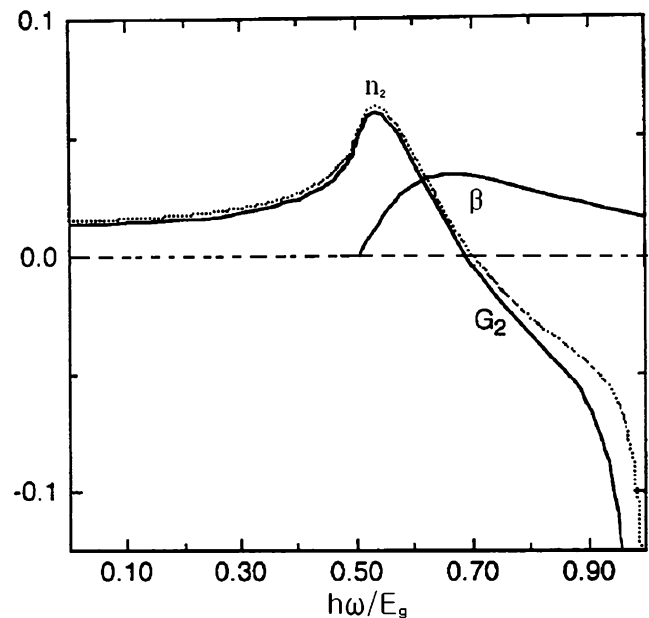


Fig. 4 Dependence of the third-order nonlinear coefficients β , n_2 (dotted line) and function G_2 (solid line) on $h\omega/E_g$

changes. $G_2(y)$ changes much faster than E_g^{-4} , therefore, the third order nonlinearity was much depressed.

On the other hand, the nonlinear absorption indexes of these samples were larger than the bulk ZnSe reported in [12]. As the wavelength of the laser is 532 nm, the incident photon energy $h\omega$ satisfies $E_g/2 < h\omega < E_g$, the TPA is permitted. So main resource of the absorption is TPA. As $h\omega/E_g \approx 0.7$, the absorption is largely induced as show in Fig. 4. The porous character of composites may also produce more absorption than ZnSe crystals. And for another, the surface of the sample had not been passivated, it may cause optical energy dissipated.

4 Conclusion

The third-order nonlinear optical indexes of the samples of ZnSe doped SiO₂ glasses were first reported. The SDGs exhibited self-defocusing character. As the doping amount increased, the third-order nonlinear coefficients augmented, too. A conclusion can be drawn that the nonlinear susceptibility could be influenced by the size and band-gap of SDGs very efficiently. These results were consistent with the local field effect and Kramers–Kronig relation. But for the samples with very small doping amount, the nonlinearity is very weak and difficult to detect. This is due to the frequency response of nonlinear refractive indexes. When $h\omega/E_g$ approaches the critical value 0.7, the sign of n_2 was changed. In order to achieve large nonlinear refractive indexes, we should design materials with $h\omega/E_g \approx 0.55$. In addition, the large absorption of SDGs

may be caused by the two photons absorption and the surface dissipation.

Acknowledgement This work was supported by the Ministry of Science and Technology of China through 973-project under grant 2002CB613305 and the Nature Science Foundation of Shannxi Province (2003E110).

References

1. G.A. Ozin, *Adv. Mater.* **4**, 612 (1992)
2. S.V. Gaponenko, *Optical Properties of Semiconductor Nanocrystal* (Cambridge University Press, Cambridge, 1998), p. 55
3. G.A. Ozin, J. Godber, A. Stein, U. S. Patent **494**, 211, (1990)
4. Yumoto, H. Shinjima, N. Uesugi, K. Tsuentomo, H. Nasu, Y. Osaka, *Appl. Phys. Lett.* **57**, 2393 (1990)
5. J. Wang, M. Sheik-bahae, A.A. Said, D.J. Hagan, E.W. Van Stryland, *J. Opt. Soc. Am. B* **11**, 1009 (1994)
6. G.R. Olbright, N. Peyghambarian, *Appl. Phys. Lett.* **48**, 1186 (1986)
7. Y.P. Wang, X. Yao, M.Q. Wang, F.T. Kong, J.F. He, *J. Cryst. Growth* **268**, 580 (2004)
8. M.Q. Wang, Y.P. Wang, et al., *Chin. Sci. Bull.* **49**, 747 (2004)
9. Y.P. Wang, M.Q. Wang, X. Yao, F.T. Kong, L.Y. Zhang, *J. Cryst. Growth* **268**, 575 (2004)
10. M. Sheik-Bahae, A.A. Said, T.H. Wei, D.J. Gagan, E.W. Van Stryland, *IEEE J. Quant. Electron.* **26**, 760 (1990)
11. H. Toda, C.M. Verber, *Opt. Lett.* **17**, 1376 (1992)
12. M. Sheik-bahae, *IEEE J. Quant. Electron.* **26**(4) (1990), April
13. X.D. Liu, S.L. Guo, *Opt. Commun.* **197**, 431 (2001)
14. S.G. Lu, Y.J. Yu, C.L. Mak, et. al., *Microelectron. Eng.* **66**, 171 (2003)
15. J. Yumoto, H. Shinjima, N. Uesugi, et. al., *Appl. Phys. Lett.* **57**, 2393 (1990)
16. M. Sheik-bahae, J. Wang, E.W. Van Stryland, *IEEE J. Quant. Electron.* **27**, 1296 (1991)